On the Formation and Dynamical Evolution of Planets in Binaries

Willy Kley[1] and Richard P. Nelson[2]

[1] Institut für Astronomie & Astrophysik, Universität Tübingen, Auf der Morgenstelle 10, D-72076 Tübingen, Germany, wilhelm.kley@uni-tuebingen.de

[2] Astronomy Unit, Queen Mary, University of London, Mile End Road, London E1 4NS, United Kingdom, r.p.nelson@qmul.ac.uk

Summary. Among the extrasolar planetary systems about 30 are located in a stellar binary orbiting one of the stars, preferably the more massive primary. The dynamical influence of the second companion alters firstly the orbital elements of the forming protoplanet directly and secondly the structure of the disk from which the planet formed which in turn will modify the planet's evolution. We present detailed analysis of these effects and present new hydrodynamical simulations of the evolution of protoplanets embedded in circumstellar disks in the presence of a companion star, and compare our results to the system γ Cep. To analyse the early formation of planetary embryos, we follow the evolution of a swarm of planetesimals embedded in a circumstellar disk. Finally, we study the evolution of planets embedded in circumbinary disks.

1 Introduction

1.1 Summary of observations

At the time of writing, approximately 29 extrasolar planets have been discovered in binary star systems, all of which are orbiting about a single component of the binary. For a review of the global statistics see the papers by Eggenberger et al. (2004) and Mugrauer et al. (2007), as well as the relevant chapters in this book (Eggenberger & Udry). So far, there have been no discoveries of circumbinary planets. The binary star systems that host planets are very diverse in their properties, with binary semimajor axes ranging from $\simeq 6400$ AU down to $\simeq 20$ AU. In the case where the orbits are eccentric, the binary periastron can be as small as $\simeq 12$ AU, such that important dynamical effects are expected to have occured during and after planet formation. One such example is the well studied system γ Cep (Hatzes et al. 2003) which contains a planet of mass $m \sin i \simeq 2$ Jupiter masses with a semimajor axis of $\simeq 2$ AU. Here the binary semimajor axis is $\simeq 18$ AU and periastron is $\simeq 12$ AU. Another interesting case is GL86 (Mugrauer & Neuhäuser 2005), which consists of a binary system whose secondary is a $\simeq 0.55$ M_{odot} white dwarf whose projected

orbital separation is $\simeq 21$ AU. GL86 is reported to host a planet with $m\,sini \simeq 4$ Jupiter masses (Queloz et al. 2000). It is worth noting that the white dwarf projenitor was probably a Solar mass main sequence star, such that the orbital separation was even smaller in the past.

Clearly the close binary systems containing planets provide an excellent laboratory for testing theories of planet formation, as the presence of the companion may create conditions normally thought to be inconducive to planet formation. It is these closer systems that we mainly focus on in this article.

1.2 Summary of planet formation in binaries

In a binary star system the early formation of planets may be strongly influenced by changes in the structure of the protoplanetary disk caused by tidal forces from the binary companion. For a circumstellar disk, significant effects will occur if the disk outer edge is tidally truncated by the binary companion, as strong spiral shock waves will be lauched near the disk edge and propagate inward. For a circumstellar disk in a binary system which is not subject to strong tidal forcing, it seems likely that the effect of the companion star will be modest, unless the orbital inclinations are such that the Kozai effect becomes important (Innanen et al. 1997). In a circumbinary disk one can almost always expect strong tidal interaction between the binary and disk, and hence significant effects on planet formation. In this article we restrict our discussion to two basic scenarios. The first is planet formation and evolution in a circumstellar disk around the primary (most massive) star - although we note that of the 29 binary systems with known planets, two of them host planets around the secondary star (16 Cyg and HD178911). The second scenario is planet formation in circumbinary disks. We restrict our discussion to those early phases of planetary formation that occur in a gas rich environment.

In a circumstellar disk, the tidal torques of the companion star generate strong spiral shocks, and angular momentum is transferred to the binary orbit. This in turn leads to disk truncation. Using analytical and numerical methods Artymowicz & Lubow (1994) show how the truncation radius r_t of the disk depends on the binary semimajor axis a_{bin}, its eccentricity e_{bin}, the mass ratio $q = M_2/M_1$ (where M_1, M_2 denote are the primary and secondary mass, respectively), and the viscosity ν of the disk. For typical values of $q \approx 0.5$ and $e_{bin} = 0.3$ the disk will be truncated to a radius of $r_t \approx 1/3 a_{bin}$ for typical disk Reynold's numbers of 10^5 (Artymowicz & Lubow 1994; Larwood et al. 1996; Armitage et al. 1999). For a given mass ratio q and semi-major axis a_{bin} an increase in e_{bin} will reduce the size of the disk while a large ν will increase the disks radius. Not only will the disk be truncated, but the overall structure may be modified by the binary companion. In section 2 we will illustrate this effect.

In a circumbinary disk, the binary creates a tidally-induced inner cavity. For typical disk and binary parameters (e.g. $e_{bin} = 0.3$, $q = 0.5$) the size of the cavity is $\simeq 2.7 \times a_{bin}$ (Artymowicz & Lubow 1994).

Whether these changes in the disk structure in circumstellar of circumbinary systems have an influence on the likelihood of planet formation in such disks has long been a matter of debate. The dynamical action of the binary has several potential consequences which may be adverse to planet formation: *i*) it changes the stability properties of orbits, *ii*) it increases the velocity dispersion of planetesimals *iii*) it reduces the life–time of the disk, and *iv*) it increases the temperature in the disk.

In a numerical study Nelson (2000) investigated the evolution of an equal mass binary with a 50 AU separation and an eccentricity of 0.3. He argued that both main scenarios of giant planet formation (i.e. through core instability or gravitational instability) are strongly handicapped, because the eccentric companion will induce a periodic heating of the disk up to temperatures possibly above 1200 K. Since the condensation of particles as well as the occurence of gravitational instability require lower temperatures, planet formation will be made more difficult. Clearly the strength of this effect will depend on the binary separation and its mass ratio. In addition to the approach taken by Nelson (2000) the influence a stellar companion has on the evolution of a massive planet embedded in a circumstellar disk has been investigated by Kley (2000), where the evolution of the embedded planet has been studied through hydrodynamical simulations (see also the review article by Kley & Burkert 2000). However, in these preliminary simulations only very short time spans have been covered and the initial disk configuration may have been unrealistic.

Recent numerical studies of the final stages of terrestrial planet formation in rather close binaries with separations of only 20–30 AU, that involve giant impacts between $\sim$ lunar mass planetary embryos, show that it is indeed possible to form terrestrial planets in such systems (Lissauer et al. 2004; Turrini et al. 2005; Quintana et al. 2007), provided it is possible for the planetary embryos themselves to form.

It is already the case for planet formation around single stars that the life–time of the disk represents a limiting factor in the formation of planets. It has been suspected that the dynamical action of a companion will reduce the life–time of disks substantially. However, a recent analysis of the observational data of disks in binary stars finds no or very little change in the lifetimes of the disks, at least for separations larger than about 20 AU (Monin et al. 2007).

The early phase of planetesimal formation and subsequent formation of Earth-like planets is described in more detail in other chapters of this book. Here we will concentrate on the formation and evolution of planets in a gas rich environment, where inclusion of the full dynamics of the protoplanetary disk is crucial. We consider the dynamics of planetesimals, low mass planets, and high mass planets in circumstellar and circumbinary disks.

2 Evolution of planets in circumstellar disks with a companion

The presence of a companion star influences the structure of a circumstellar disk around the primary star due to gravitational torques acting on the disk. This leads to an exchange of energy and angular momentum between the binary and the disk. For close binaries the disk becomes truncated where the truncation radius r_t depends primarily on the parameters of the binary, i.e. the mas ratio q, the semi-major axis a_{bin} and eccentricity e_{bin}, and the viscosity of the disk. The radius r_t has been calculated semi-analytically and numerically by Artymowicz & Lubow (1994).

The effects of the companion on planet formation are likely to be most pronounced in binaries with separations ≤ 20 AU, rather than in long period systems with $a_{bin} > 1000$ AU. Among the very close binary stars containing planets is the well studied system γ-Cep. Including observations taken over decades, Hatzes et al. (2003) confirmed the presence of a planet orbiting the primary star in this system.

Very recently, new radial velocity measurements and additional Hipparcos data have refined the binary orbit (Torres 2007) and the direct imaging of the secondary has fixed the masses of the binary to $M_1 = 1.4$ and $M_2 = 0.4 M_\odot$ (Neuhäuser et al. 2007). This system with a binary separation of about 20 AU contains a massive planet with a minimum mass of $1.6 M_{Jup}$ orbiting the primary star at a distance of approximately 2.1 AU. Assuming that the planet has not been captured at a later time, or that the binary orbit has not shrunk since planet formation, this system represents a very challenging environment for the formation of planets indeed, and we choose it to illustrate the main influence a close companion has on the planet formation process.

2.1 Disk evolution in the presence of a companion

When studying the formation of planets in a protoplanetary disk in the presence of a secondary star it is necessary to first follow the evolution of the perturbed disk without an embedded planet and bring the system into equilibrium, before adding a planetary embryo at a later time.

We choose to model a specific system where the orbital elements of the binary have been chosen to match the system γ Cep quite closely. The data for this system have been taken from (Hatzes et al. 2003) which do not include the most recent improvements mentioned above (Neuhäuser et al. 2007). These newest refinements primarily concern the mass of the primary and do not alter our conclusions at all. We are interested here in demonstrating the principle physical effects rather than trying to achieve a perfect match with all the observations of this particular system.

For this study we choose a binary with $M_1 = 1.59 M_\odot$, $M_2 = 0.38 M_\odot$, $a_{bin} = 18.5$ AU and $e_{bin} = 0.36$, which translates into a binary period of $P = 56.7$ yrs. We assume that the primary star is surrounded by a flat circumstellar disk, where the binary orbit and the disk are coplanar. In a numerical hydrodynamical model of the system, the fact that the disk's vertical thickness $H(r)$ at a given distance r from the primary is typically small with respect to the radius ($H/r << 1$) is typically used to perform restricted two-dimensional (2D) simulations and neglect the vertical extent altogether. Here, we present such 2D hydrodynamical simulations of a circumstellar disk which is perturbed by the secondary. We assume that the effects of the intrinsic turbulence of the disk can be described approximately through the viscous Navier-Stokes equations, which are solved by a finite volume method which is second order in space and time. To substantiate our results we utilize two different codes `RH2D` (Kley 1999, 1989) and `NIRVANA` (Nelson et al. 2000; Ziegler & Yorke 1997).

Numerical Setup: As the disk is orbiting only one star we utilize an adapted cylindrical coordinate system (r, φ) which is centered on the primary. It extends radially from $r_{min} = 0.5$ AU to $r_{max} = 8$ AU and in azimuth around a whole annulus ($\varphi_{min} = 0, \varphi_{max} = 2\pi$). Within this domain at the beginning of the simulations ($t = 0$) an axisymmetric disk (with respect to the primary) is initialized with a surface density profile $\Sigma(r) = \Sigma_0 r^{-1/2}$ where the reference density Σ_0 is chosen such that the total mass in the compuational domain (within r_{min} and r_{max}) equals $1.75 \cdot 10^{-3} M_\odot$ which implies $\Sigma_0 = 1.89 \cdot 10^{-5} M_{sol}/\mathrm{AU}^2$. The temperature profile is fixed here and given by $T(r) \propto r^{-1}$ which follows from the assumed constancy of $h = H/r$ which is fixed to $h = 0.05$. For the viscosity we assume an α-type prescription where the coefficient of the kinematic viscosity is given by $\nu = \alpha c_s H$ with $\alpha = 0.005$, and the sound speed $c_s(r) = h\, v_{kep}(r)$.

The boundary conditions are chosen such that material may escape through the radial boundaries. At the outer boundary (r_{max}) we impose a so called zero-gradient outflow condition. During periastron when large spirals may extend beyond r_{max} this condition will allow material to leave the system and not create numerical artifacts. At the inner boundary we set a viscous outflow condition where the material may flow through r_{min} with the local (azimuthally averaged) viscous inflow referring to an accretion disk in equilibrium. No matter is allowed to flow back into the system and the mass of the disk will slowly decline. To ensure a uniform setup for the planets we rescale the disk mass when inserting them.

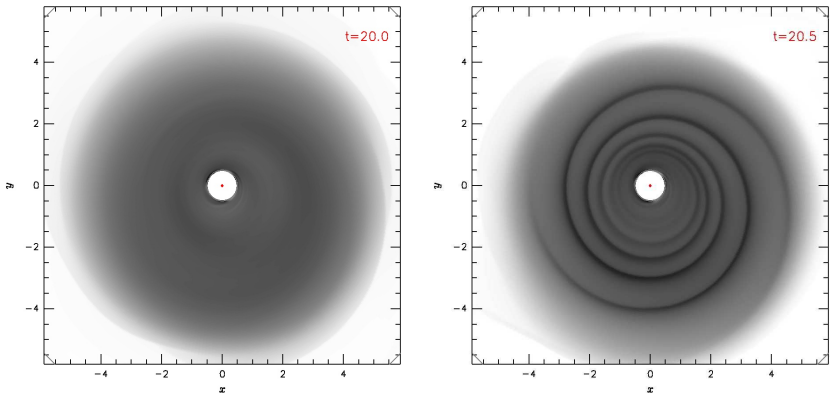

Fig. 1. Grayscale plot of the two-dimensional density distribution of the circumstellar disk around the primary at two different orbital phases of the binary. **Left** shortly after apocente at about 20 binary orbits, and **Right** shortly after closest approach (pericentre).

The structure of the disk

The presence of an eccentric secondary star leads to a strong periodic disturbance of the disk whenever it is at periastron. Two strong spiral arms (shock waves) are created in the disk which carry material beyond the outer boundary of the computational domain. In between the periapses the disk settles down and becomes more circular again. This effect is illustrated in the Fig. 1 where we display the surface density Σ of the disk in gray scale at 2 different times in the early evolution of the disk, see also Nelson (2000). Already the very first approaches with the binary lead to a truncation of the disk as visible in left panel of Fig. 2 for the curve at $t = 10$ binary orbits. Slowly the whole disk structure rearranges and equilibrates at around $t = 50$ where it shows a much steeper density slope than in the intial state. The timescale for this equilibration process depends on the magnitude of the disk viscosity. The eccentricity of the disk in the final state of the disk varies approximately between 0.1 and 0.16 depending on the position of the binary in its orbit as shown in the left panel of Fig. 3. The disk eccentricity $e_{disk}(r)$ has been obtained by

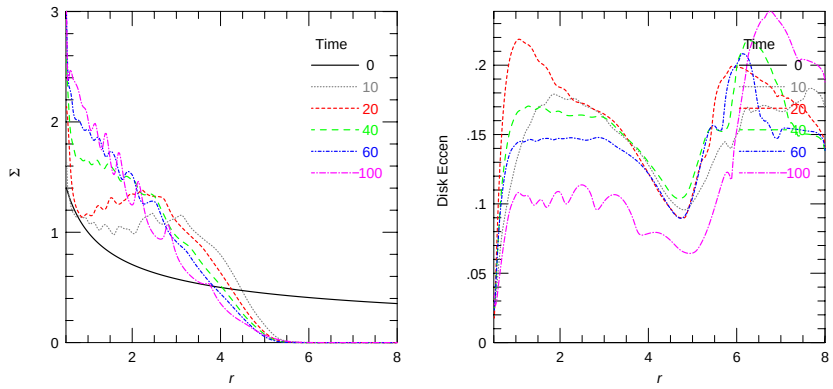

Fig. 2. The radial surface density distribution (**Left**) and the eccentricity (**Right**) of the circumstellar disk around the primary in the presence of the secondary. Time is given units of the binary orbit, radial distance in AU, and the density in dimensionless units.

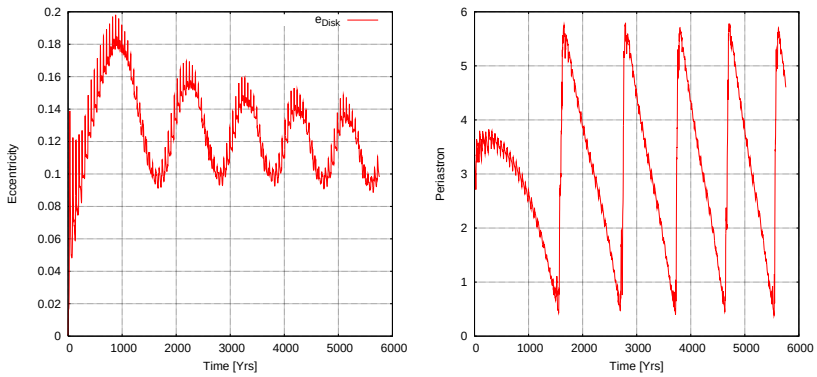

Fig. 3. The evolution of the global mass averaged disk eccentriticy (**left**) and the position angle of the disk's periapse (**right**).

calculating the eccentricity of each disk element, as if in a two body motion with the primary star, and then averaged over the respective annulus. At the same time the disk as a whole precesses as is shown in the right panel of Fig. 3. This coherent slow retrograde precession with a pattern speed much smaller than the orbital period of the disk material around the star is caused by the non-negligible pressure forces operating in the disk. Similar behaviour has been demonstrated for disks with free eccentricity (Papaloizou 2005).

The orbital elements of the binary

In the previous section we have seen that the gravitational torques of the binary lead to a truncation of the disk and re-arrangement of the material within. In turn, we expect a change in the orbital elements of the binary.

To estimate theoretically the magnitude of the back reaction a circumstellar disk has on the orbital elements of the binary during the initial phase of readjustment, we assume an idealized system consisting of a binary system and a ringlike mass distribution orbiting star 1 with mass m_{ring}, at a distance (δ-function) of r_{ring}. The energy E_{bin} and angular momentum L_{bin} of the binary is given by

$$E_{bin} = -\frac{GM\mu}{2a_{bin}}, \quad L_{bin} = \mu \left(GMa_{bin}\left(1-e_{bin}^2\right)\right)^{1/2}, \tag{1}$$

and the corresponding quantities of the ring are

$$E_{ring} = -\frac{GM_1 m_{disk}}{2r_{ring}}, \quad L_{ring} = m_{ring}\left(GM_1 r_{ring}\right)^{1/2}, \tag{2}$$

where $M = M_1 + M_2$ is the total mass of the two stars and $\mu = M_1 M_2/M$ is the reduced mass. Now, suppose that the ring is shifted from its initial position r_{ring}^{α} to a smaller radius r_{ring}^{β} keeping all its mass. This radius change mimicks the initial truncation of disk by the binary. Through this process the ring's energy and angular momentum are reduced from E_{ring}^{α} and L_{ring}^{α} to E_{ring}^{β} and L_{ring}^{β}. By conservation of total enery and angular momentum

$$E = E_{ring} + E_{bin} \quad L = L_{ring} + L_{bin}, \tag{3}$$

we can calculate the corresponding change in the orbital elements of the binary from E_{bin}^{α} and L_{bin}^{α} to E_{bin}^{β} and L_{bin}^{β}. For the binary paramter masses $M_1 = 1.6M_{\odot}, M_2 = 0.4\odot$ with initial orbital elements $a_{bin}^{\alpha} = 18.5$AU and $e_{bin}^{\alpha} = 0.36$ we find for the shift of a ring with $m_{ring} = 4{\cdot}10^{-3}M_{\odot}$ and initial radius $r_{ring}^{\alpha} = 4.0$AU to a final radius of $r_{ring}^{\beta} = 2.0$AU that the binary elements change to $a_{bin}^{\beta} = 19.4$AU and $e_{bin}^{\beta} = 0.41$. A quite substantial change considering the smallness of the ring's mass in comparision to the stellar masses. But the closeness to the primary allows to gain a substantial amount of binding energy from the ring. The calculation is approximate in the sense that the energy and angular momentum of the ring are calculated with respect to the non-inertial coordinate frame centered on the primary.

We can now compare this estimate with the previous hydrodynamical simulations and plot in Fig. 4 the evolution of a_{bin} and e_{bin} for about the first 100 binary periods with no planet included. As demonstrated above, the binary expands as it gains energy from the compressed disk and increases its eccentricity. The increase in e_{bin} does not lead to a decrease in the angular momentum however, since it increases its separation, see Eq. 1. Whenever the binary is near periastron the gravitational interaction with the disk is maximal which results in the strong periodic spikes in the binary elements. The change in the orbital elements of the binary is somewhat smaller than the estimated values because *i*) the mass of disk is smaller in the hydrodynamic calculation and *ii*) disk mass and angular momentum are stripped off by the secondary and are lost through the outer boundary of the computational domain. The loss through the (open) inner boundary of the disk is only marginal.

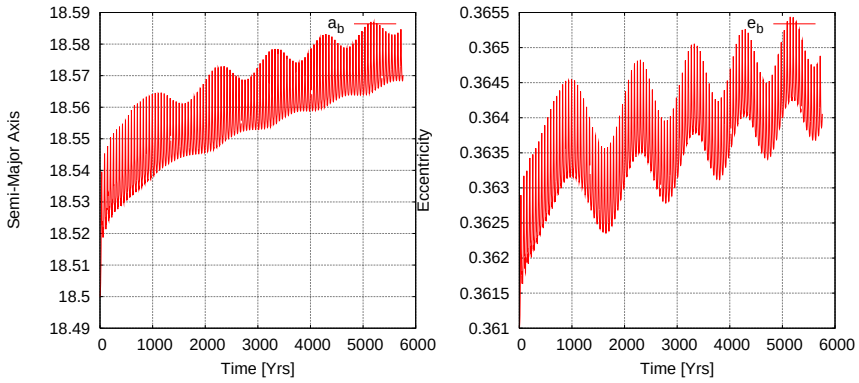

Fig. 4. The evolution of the binary elements due to the interaction with the circumstellar disk around the primary star, without an embedded planet. One binary orbit refers to approximately 57yrs. **Left**: $a_{bin}(t)$; **Right**: $e_{bin}(t)$.

The behaviour of an embedded planet

In the previous section we have seen that the gravitational torques of the binary lead to a truncation of the disk and a rearrangement of the disk material. To study the influence of the companion on the evolution of small protoplanets we embed, after an equilibration time of 100 binary orbits (nearly 6000 yrs), a $30 M_{Earth}$ planet in the disk and follow its subsequent evolution. This rather time consuming procedure to generate the initial state is necessary to obtain realistic initial conditions for the growing protoplanet. At the time of insertion of the planet the remaining disk mass is rescaled to contain 3 M_{Jup} within the computational domain.

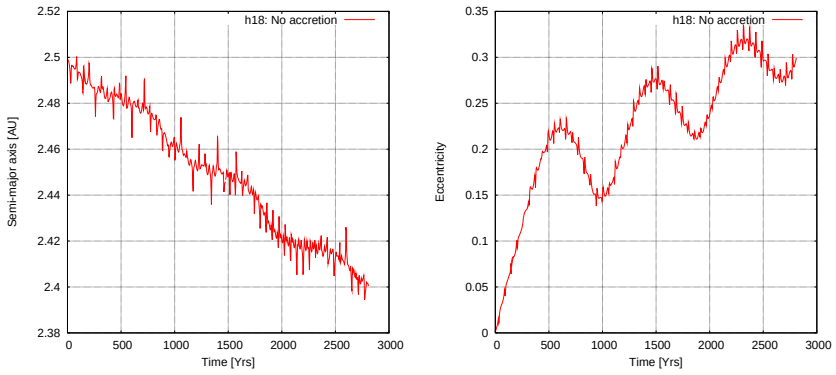

Fig. 5. The evolution of the semi-major (**left**) axis and eccentricity (**right**) of an embedded planet in the circumstellar accretion disk. Here, the planet is not allowed to accrete material from the disk and remains at 30 M_{Earth}. The planet is inserted after 100 orbital binary periods, and the time is reset to zero.

As a first sample case we follow the planet's orbital evolution while keeping its mass constant, i.e. the planet is not allowed to accrete mass from its environment. This model will serve as a reference for the subsequent cases which will allow for planetary mass growth. The planet is released at $a_p = 2.5$AU on a circular orbit. After insertion of the planet its orbital elements will change due to gravitational interaction with the disk and the binary. The planet migrates inward due to the torques of the disk, with a rate of 0.1 AU in about 2800 yrs. While the overall migration is approximately linear over this time, it is modulated by the binary companion and the precessing, eccentric disk (see left panel of Fig. 5). At the same time the planetary eccentricity increases to about 0.3, with the eccentric disk yielding the prime contribution to the growth of e_p. The oscillatory behaviour originates from the changing degree of apsidal alignent between eccentric disk and planet as they undergo relative precession.

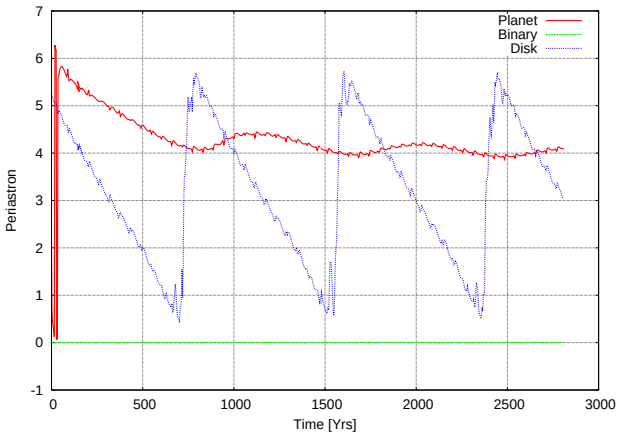

Fig. 6. The evolution of the argument of pericenter of the disk, the planet and the binary after insertion of a 30 M_{Earth} planet.

The evolution of the argument of pericenter of the disk, the planet and the binary are displayed in Fig. 6. While the disk continues its retrograde precession and the binary remains unchanged, the planet undergoes initially a retrograde precession and then settles to an approximately constant value with oscillations whose frequency is given by the precession frequency of the whole disk in which it is embedded.

To study more realistic cases we now allow the planet to grow in mass from the disk during its motion through it. The accretion process is modelled numerically in a simple manner. At each time step a certain fraction of the material within the Roche lobe of the planet is taken out of the computational domain and added to planet's mass. In Fig. 7 we show the evolution of the mass of the planet for different accretion rates. For the largest accretion rates the planet aquires over $1.8 M_{Jup}$ within the first 700 yrs of its evolution, a value that is unrealistically high. So this model sets the limiting case for the others. The model with the small accretion only doubles its mass from 30 to 60 M_{Earth} during the first 1000 yrs which gives a more realistic accretion rate. The no accreting case is given by the horizontal line.

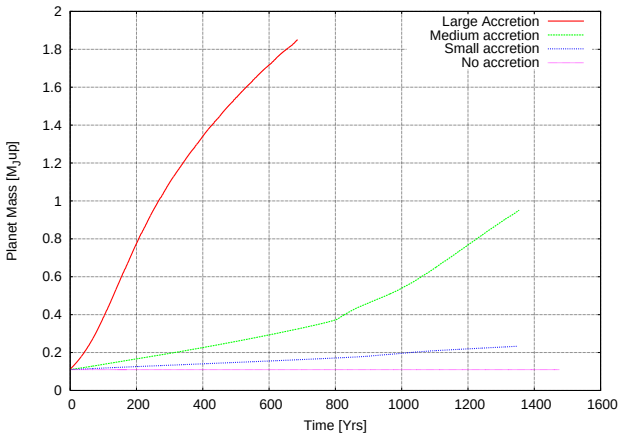

Fig. 7. The evolution of the argument of pericenter of the disk, the planet and the binary after insertion of a 30 M_{Earth} planet. The planets are inserted after 100 orbital binary periods, and the time is reset to zero.

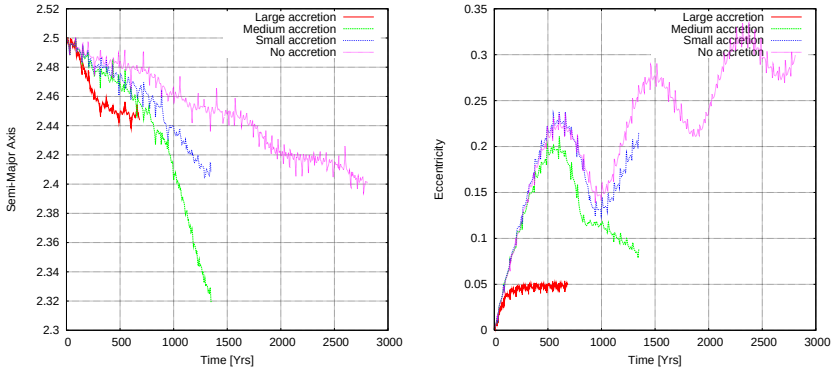

Fig. 8. The evolution of the semi-major (**left**) axis and eccentricity (**right**) of embedded planets in the circumstellar accretion disk. The planets all start at the same mass but accrete at different rates from the accretion disk. The planets are inserted after 100 orbital binary periods, and the time is reset to zero.

More interesting is now the different orbital behaviour of the planets which is displayed in Fig.8. The planet with the constant mass has the slowest migration, and the larger the accretion rate the larger is the migration speed. This is consistent with the estimated migration rates for different masses (D'Angelo et al. 2003). The planet with the maximum accretion rate grows rapidly in mass and approaches already after 280 yrs the 1 M_{Jup} limit, when its migration rate slows down and levels off as the mass in the disk decreases and the driving agent disappears. The intermediate cases migrate initially with the same speed as the non-accreting model but accelarate as the planetary mass increases.

Concerning the eccentricity evolution, the lightest planet experiences the largest growth. For the large accretion rate the eccentricity soon levels off to a value of $e_p = 0.05$.

Comparison with γ Cep

The most up to date observational data suggest the following parameters for the planet in the γ Cep system: $a_p \simeq 2.044$, $e_p \simeq 0.115$ and $m_p \sin i \simeq 1.60$ $M_{Jupiter}$. If this planet formed according to the core instability model, then our simulations raise a number of important questions that we are currently addressing.

First, a low mass, non accreting planet embedded in an the eccentric disk experienced substantial growth in eccentricity (see Fig. 5). This has clear implications for the accretion of planetesimals because their velocity dispersion may become very large due to this effect. Thébault et al. (2004) examined the evolution of planetesimal orbits under the influence of the binary companion and aerodynamical gas drag. They concluded that accretion of planetesimals would occur in the shear dominated regime because orbital alignment was maintained due to the gas drag. This work, however, did not include the effects of an eccentric disk, and so it remains unclear whether planetesimal orbits will remain aligned. We will discuss the effects of including the full dynamics of the disk when calculating the orbital evolution of planetesimals in the γ Cep system in the next section.

A second issue is that of type I migration of the giant planet core that must survive before gas accretion occurs. Fig. 5 shows the non accreting, low mass planet undergoing quite rapid inward migration. The migration, however, is modulated by the eccentricity of the planet, such that at high eccentricity phases the migration rate decreases. It is possible that longer run times will show an essential stalling of this migration if the planet eccentricity grows beyond its final value of $e_p \simeq 0.3$. Simulations are currently being conducted to examine this in more detail.

Once gas accretion is switched on, it is clear that a disk mass of about 3 Jupiter masses, where the outer disk radius is tidally truncated at $r \simeq 5$ AU, will be sufficient to grow a planet that is close to the minimum observed mass of $m_p \sin i \simeq 2.044$ $M_{Jupiter}$. It is also clear that we can construct a model in which a low mass planet growing from an initially circular orbit can achieve a final mass of $m_p \simeq 2$ $M_{Jupiter}$, and have a final eccentricity of $e_p \simeq 0.1$ as required. Calculations are underway to see if a planetary core on an initially eccentric orbit (as expected from Fig. 5), will circularise as it accretes gas from the disk such that a self consistent model that fits the observations can be constructed.

A final comment relates to the final mass of the planet. Our simulations suggest that a disk mass of about 3 Jupiter masses will be enough to form a gas giant of the required miminum mass. A future test of the mode by which the planet in γ Cep formed (gravitational instability versus core accretion) will be determination of its actual mass. We suspect that a disk that is massive enough to form a planet through gravitational unstability will lead to a planet whose final mass is substantially larger than the minimum value observed.

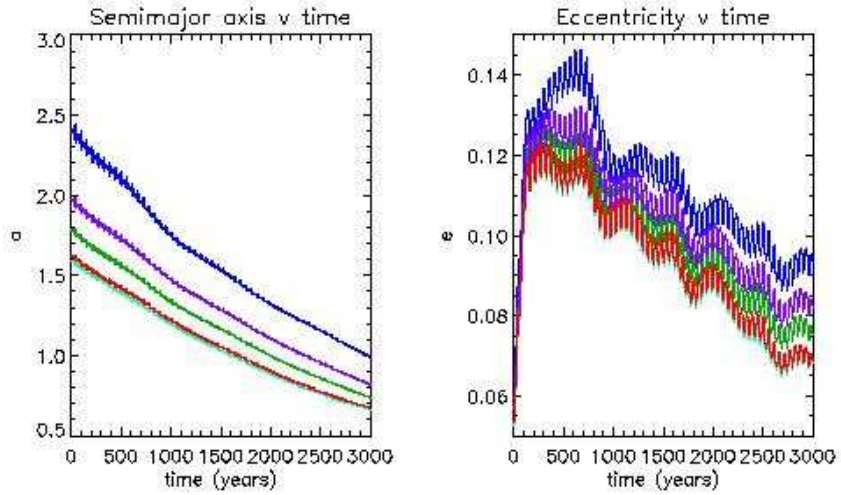

Fig. 9. The evolution of the semi-major axes (left panel) and eccentricities (right panel) of embedded planetesimals in the circumstellar accretion disk.

3 Evolution of planetesimals in a circumstellar disk with a companion

We now describe preliminary results from simulations of planetesimals embedded in circumstellar disks with a companion star. We take as our basic model the disk and binary system described in the previous section 2. As in the models in which low mass protoplanets were considered, we evolve the system for 100 binary orbits prior to inserting 100 planetesimals. At the point when the planetesimals are inserted, the disk mass is augmented so that it contains 3 Jupiter masses in total. The planetesimals are randomly distributed initially between orbital radii of 1.5 and 2.5 AU on circular Keplerian orbits. We consider here planetesimals whose physical radii are 100 metres. A broader range of sizes will be discussed in Nelson & Kley (2007, in preparation). The planetesimals experience aerodynamic gas drag using the standard formulae found in Weidenschilling (1977), and also experience the gravitational force due to the disk, central star and companion star. Although the simulations we describe here are two dimensional, we assume that the planetesimals lie in the disk midplane and calculate the volumetric density from the surface density by assuming that the vertical density profile is Gaussian with scale height $H = 0.05r$, where r is the orbital radius. We use linear interpolation to calculate the gas density and velocity at the planetesimal positions for use in the gas drag formula. The evolution of the semi-major axes and eccentricities for 5 representative planetesimals are shown in figure 9. We see that the planetsimals migrate inward on the expected time scale due to the aerodynamic gas drag, and are also excited onto orbits with high eccentricity ($e \geq 0.12$). The eccentricity is driven upward primarily by gravitational interaction with the eccentric gas disk, and not because of direct interaction with the binary companion. As the planetesimals drift inward their eccentricity decays slightly but still remains significant.

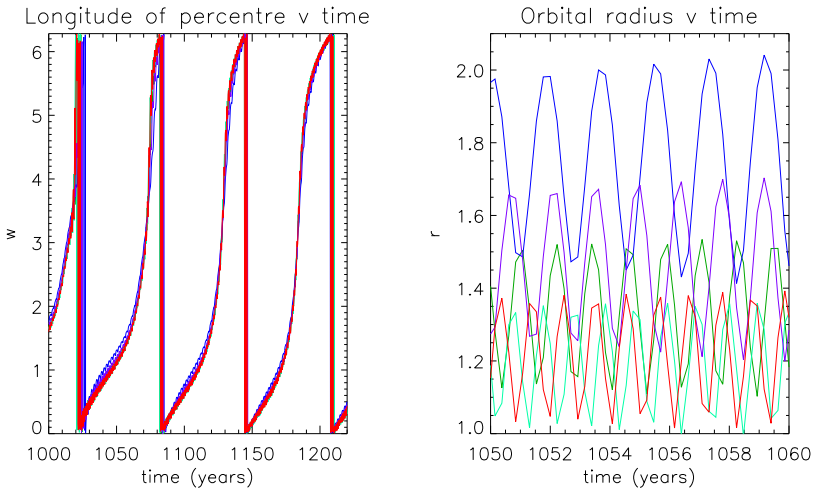

Fig. 10. The evolution of the longitudes of pericentre (left panel) and orbital radii (right panel) of embedded planetesimals in the circumstellar accretion disk. Notice that the orbits cross one another, suggesting that high velocity impacts are likely to occur.

In the left panel of figure 10 we plot the longitude of pericentre of the five representative planetesimals for times between 1000 and 1200 years after the planetesimals were inserted. We see that their orbits remain quite close to alignment, but the alignment is not perfect and the degree of alignment is time dependent. The right panel shows the orbital radii of the five planetesimals, and we see clearly that the orbits cross. Given eccentricities on the order of $e \simeq 0.1$ and semimajor axes approximately $a \simeq 1.5$ AU, this suggests that collision velocities between the planetesimals will be on the order of 2 km s^{-1}. Simulations of colliding icy bodies with radii $\simeq 100$ m performed by Benz & Asphaug (1999) suggest that disruption occurs for impact velocities $\simeq 15$ m s^{-1}, a factor of $\simeq 1/133$ smaller than the velocity dispersions obtained in our simulations. Clearly this raises questions about the applicability of the core instability model when applied to close binary systems such as γ Cep, as it would appear that impacts between planetesimals will be destructive rather than accretional.

4 Evolution of planets in circumbinary disks

In this section we present the results of simulations that examine the evolution of both low and high mass protoplanets which form in circumbinary disks. A fuller discussion of the work relating to low mass planets is presented in Pierens & Nelson (2007), and a detailed description of the simulations relating to high mass planets is presented in Nelson (2003).

We consider the interaction between a coplanar binary and protoplanet system and a two–dimensional, gaseous, viscous, circumbinary disk within which it is sup-

posed the protoplanets form. We do not address the formation process itself, but rather assume that circumbinary protoplanets can form, and examine the dynamical consequences of this. Each of the stellar components and the protoplanet experience the gravitational force of the other two, as well as that due to the disk. The planet and binary orbits are evolved using a fifth–order Runge–Kutta scheme (Press et al. 1992). The force of the planet on the disk, and of the disk on the planet, is softened using a gravitational softening parameter $b = 0.5a_p(H/r)$, where a_p is the semimajor axis of the planet, and H/r is the disk aspect ratio. We assume that the mass of the protoplanet is fixed, and disk models have effective aspect ratio $H/r = 0.05$.

4.1 Low mass circumbinary planets

The simulation described below was performed using the hydrodynamics code `GENESIS` (Pierens et al. 2005; de Val-Borro et al. 2006). The Shakura–Sunyaev viscosity parameter $\alpha = 2 \times 10^{-4}$, and the disk was initialised to have a mass of 0.04 $M_\odot$ within a radius of 40 AU. An expanded version of the following discussion is presented in Pierens & Nelson (2007).

The simulation was initialised with a binary star system on a circular orbit surrounded by an unperturbed circumbinary disk. The stellar masses were $M_1 = 1/11 M_\odot$ and $M_2 = 1/110 M_\odot$ (i.e. the mass ratio was $q = 0.1$), and the semimajor axis $a_{bin} = 0.4$ AU. The left panel of figure 11 shows the slow decline of the binary semimajor axis over a time scale of about 80,000 years (the binary orbital period is approximately 92 days) and the right panel shows the growth and saturation of the binary eccentricity. As expected, interaction with the disk drives the growth of binary eccentricity (e.g. Papaloizou, Nelson & Masset 2001), which eventually saturates at a value of $e_{bin} \simeq 0.08$.

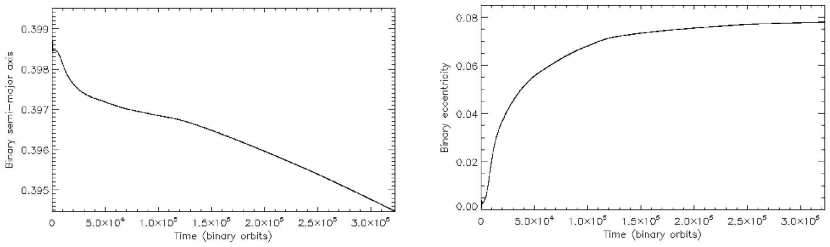

Fig. 11. The evolution of the binary elements due to interaction with the circumbinary disk. The left panel shows the semimajor axis evolution over time (expressed in binary orbits), and the right panel shows the eccentricity evolution. The binary orbital period is ~ 92 days.

Once the binary eccentricity reaches a constant value, a low mass protoplanet ($m_p = 50\ M_\oplus$) was inserted in the disk on a circular orbit with semimajor axis $a_p = 3$ AU and allowed to evolve. The planet migrates inward due to interaction with the disk, as shown in figure 12, which also shows the planet eccentricity evolution. As the planet semimajor axis reaches a value of $a_{bin} \simeq 1.1$ AU, we see that migration

suddenly stalls. This halting of migration appears to be robust, and occurs for planets whose masses that are too small for gap formation in the gas disk to occur (Pierens & Nelson 2007 - in preparation). We ascribe this beviour to an increase in the corotation torque as the planet enters the inner cavity that is cleared by the tidal torques of the binary. A similar effect has been described by Masset et al. (2006) who show that planet migration can be halted due to the action of corotation torques at surface density transitions. As such, we expect this stalling of migration for low mass planets to be a generic feature within circumbinary disks, and to occur near the edge of the tidally truncated cavity generated by the binary. The left panel of figure 13 shows the azimuthally averaged surface density in the disk as a function of radius at the end of the simulation, and illustrates the point that the planet stalls within the inner cavity due to corotation torques. The right panel shows an image of the binary, protoplanet and circumbinary disk at the end of the simulation.

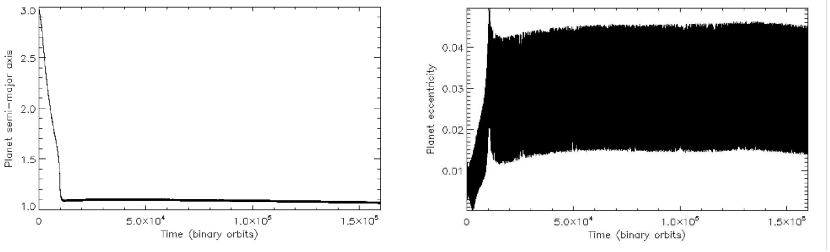

Fig. 12. The evolution of the planet elements due to interaction with the circumbinary disk. The left panel shows the semimajor axis evolution over time in years, and the right panel shows the eccentricity evolution.

4.2 High mass circumbinary planets

The simulations described below were evolved using the hydrodynamics code `NIRVANA` (Ziegler & Yorke 1997). The viscosity parameter $\alpha = 5 \times 10^{-3}$, and the surface density was normalised such that the disk contains about 4 Jupiter masses interior to the initial planet semimajor axis (Nelson 2003).

The total mass of the binary plus protoplanet system is assumed to be 1 $M_{\odot}$. We use units in which the gravitational constant $G = 1$, and the unit of length is approximately 3.6 AU. The initial binary semimajor axis is $a_{bin} = 0.4$ in our computational units, and the initial planet semimajor axis $a_p = 1.4$, corresponding to 5 AU in physical units. Thus the planet lies just outside the 6:1 mean motion resonance with the binary. Simulations were performed for a variety of initial binary eccentricities, e_{bin}, and the protoplanet was initially in circular orbit. The binary mass ratio $q_{bin} = 0.1$ for all simulations presented in this section, but larger values were considered in Nelson (2003). The unit of time quoted in the discussion below is the orbital period at $R = 1$.

The results of the simulations can be divided into three main categories (Mode 1, Mode 2, and Mode 3), which are described below, and are most strongly correlated

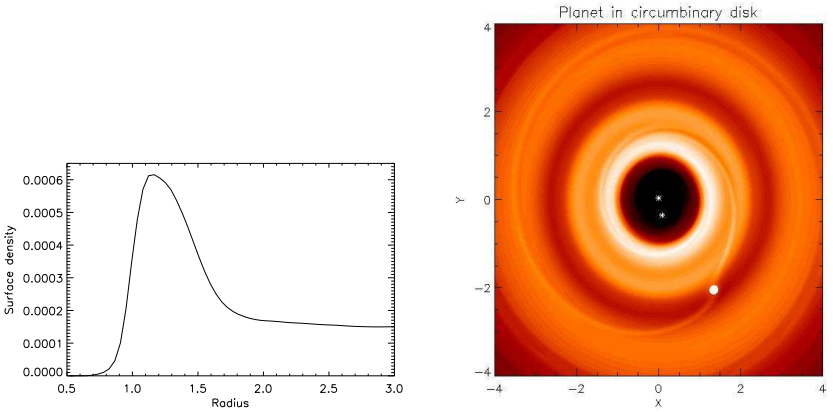

Fig. 13. The left panel shows the azimuthally averaged surface density profile at the end of the simulation. The right panel shows an image of the disk along with the protoplanet and binary system. This image corresponds to an earlier time during which the planet is migrating inward toward the central binary system.

with changes in the binary mass ratio, q_{bin}, and binary eccentricity e_{bin}. Changes to the disk mass and/or protoplanet mass appear to be less important. Here we present the results of just three simulations that illustrate these basic modes of evolution.

In some runs the planet entered the 4:1 mean motion resonance with the binary. The associated resonant angles in the coplanar case are defined by:

$$\begin{aligned} \psi_1 &= 4\lambda_s - \lambda_p - 3\omega_s \qquad & \psi_2 &= 4\lambda_s - \lambda_p - 3\omega_p \\ \psi_3 &= 4\lambda_s - \lambda_p - 2\omega_s - \omega_p & \psi_4 &= 4\lambda_s - \lambda_p - 2\omega_p - \omega_s \end{aligned} \tag{4}$$

where λ_s, λ_p are the mean longitudes of the secondary star and protoplanet, respectively, and ω_s, ω_p are the longitudes of pericentre of the secondary and protoplanet, respectively. When in resonance ψ_3 or ψ_4 should librate, or all the angles should librate. In principle the protoplanet is able to enter higher order resonances than 4:1, such as 5:1 or 6:1, since its initial location lies beyond these resonance locations. However, none of the simulations presented here resulted in such a capture. Test calculations indicate that capture into higher order resonances requires slower planetary migration rates than those that arise in these simulations. For significantly faster migration rates the planet may pass through the 4:1 resonance (Nelson 2003).

Mode 1 – Planetary Scattering

A number of simulations resulted in a close encounter between the protoplanet and binary system, leading to gravitational scattering of the protoplanet to larger radii, or into an unbound state. We label this mode of evolution as 'Mode 1'. Typically the initial scattering causes the eccentricity of the planet to grow to values $e_p \simeq 0.9$, and the semimajor axis to increase to $a_p \simeq 6 - 8$. In runs that were continued for significant times after this initial scattering, ejection of the planet could occur after subsequent close encounters.

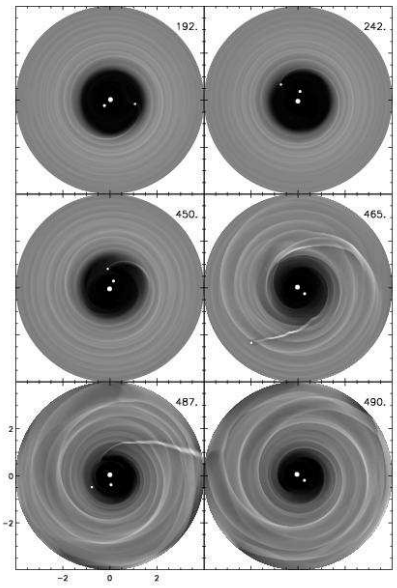

Fig. 14. This figure shows surface density contours for run in which the planet is ejected by the binary

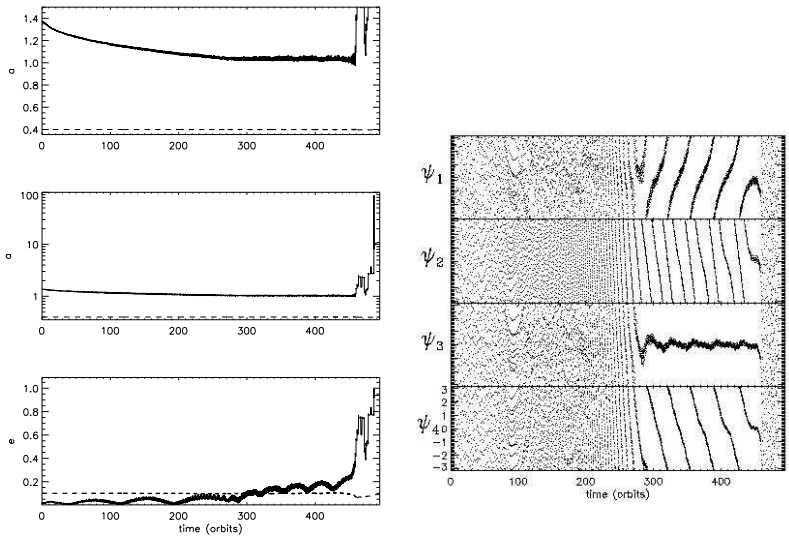

Fig. 15. The left panel shows the semimajor axes and eccentricities for a run in which planet is scattered by the binary. The right panel shows the resonant angles for the 4:1 resonance, indicating capture into this resonance prior to scattering.

We illustrate this mode of evolution using a simulation with $m_p = 3$ Jupiter masses and $q_{bin} = 0.1$. A series of snapshots of the simulation are shown in figure 14. Mode 1 evolution proceeds as follows. The protoplanet migrates in toward the central binary due to interaction with the circumbinary disk, and temporarily enters the 4:1 mean motion resonance with the binary. The migration and eccentricity evolution is shown in the left panel of figure 15, and the resonance angles are shown in the right panel. The resonant angle ψ_3 librates with low amplitude, indicating that the protoplanet is strongly locked in the resonance. The resonance drives the eccentricity of the protoplanet upward, until the protoplanet has a close encounter with the secondary star during or close to periapse, and is scattered out of the resonance into a high eccentricity orbit with significantly larger semimajor axis. We note that the existence of a resonance normally helps maintain the stability of two objects orbiting about a central mass. However, when one of the objects is a star, the large perturbations experienced by the planet can cause the resonance to break when the eccentricities are significant. Once out of resonance, the chances of a close encounter and subsequent scattering are greatly increased. This provides a method of forming 'free–floating planets'.

Mode 2 – Near–resonant Protoplanet

A mode of evolution was found in some of the simulations leading to the protoplanet orbiting stably just outside of the 4:1 resonance. We label this mode of evolution as 'Mode 2'. Mode 2 evolution is illustrated by a simulation for which $m_p = 1$, $q_{bin} = 0.1$, and $e_{bin} = 0.1$. The evolution of the orbital elements are shown in figure 16. Here, the protoplanet migrates inward and becomes *weakly* locked into the 4:1 resonance, with the resonant angle ψ_3 librating with large amplitude. The resonance becomes undefined and breaks when $e_p = 0$ momentarily during the high amplitude oscillations of e_p that accompany the libration of ψ_3. The protoplanet undergoes a period of outward migration through interaction with the disk by virtue of the eccentricity having attained values of $e_p \simeq 0.17$ once the resonance is broken. Unpublished simulations show that gap–forming protoplanets orbiting in tidally truncated disks undergo outward migration if they are given eccentricities of this magnitude impulsively. The outward migration moves the planet to a safer distance away from the binary, helping to avoid instability.

Once the protoplanet has migrated to just beyond the 4:1 resonance the outward migration halts, since its eccentricity reduces slightly, and the planet remains there for the duration of the simulation. The system achieves a balance between eccentricity damping by the disk and eccentricity excitation by the binary, maintaining a mean value of $e_p \simeq 0.12$ (Nelson 2003). The torque exerted by the disk on the protoplanet is significantly weakened by virtue of the finite eccentricity (Nelson 2003), preventing the planet from migrating back toward the binary.

Continuation of this run in the absence of the disk indicates that the planet remains stable for over 6×10^6 orbits. This is in good agreement with the stability criteria obtained by Holman & Wiegert (1999) since the protoplanet lies just outside of the zone of instability found by their study.

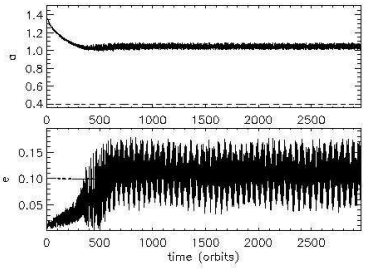

Fig. 16. This figure shows semimajor axes and eccentricities for the Mode 2 run described in the text.

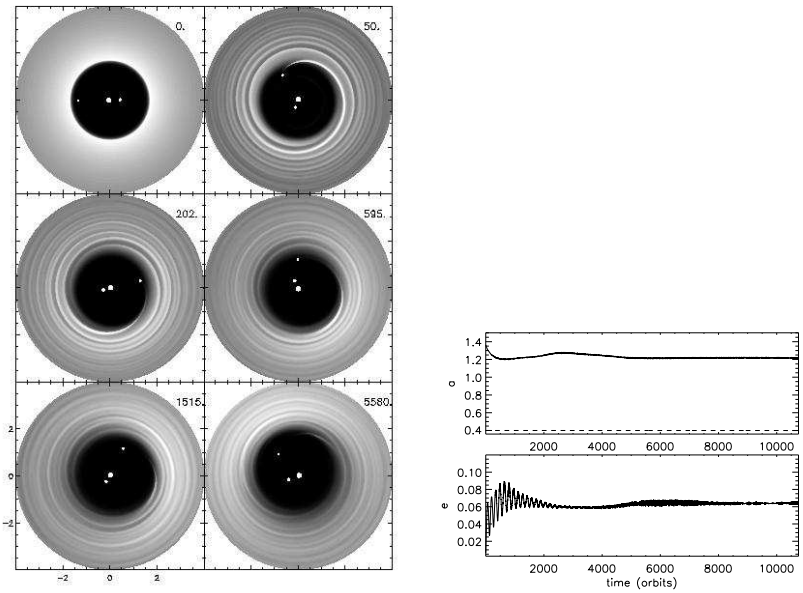

Fig. 17. The left panel shows contours of surface density for the Mode 3 run described in the text. The right panel shows the resulting changes to the semimajor axis and eccentricity of the protoplanet.

Mode 3 – Eccentric Disk

A mode of evolution was found in which the planetary migration was halted before the protoplanet could approach the central binary and reach the 4:1 resonance. This only occurred when the central binary had an initial eccentricity of $e_{bin} \geq 0.2$. The migration stalls because the circumbinary disk becomes eccentric. We label this mode of evolution as 'Mode 3', and illustrate it using a simulation with $m_p = 1$ Jupiter mass, $q_{bin} = 0.1$, and $e_{bin} = 0.2$. The left panel of figure 17 shows snapshots of the surface density at different times during the simulation, with the disk becoming noticeably eccentric. Interaction between the protoplanet and the eccentric disk leads to a dramatic reduction or even reversal of the time–averaged torque driving the migration. This is because the disk–planet interaction becomes dominated by the $m = 1$ surface density perturbation in the disk rather than by the usual interaction at Lindblad resonances in the disk. Linear calculations of planets orbiting in eccntric disks also show the possibility of outward or stalled migration (Papaloizou 2002).

The right panel of figure 17 shows the evolution of the semimajor axis and eccentricity of the planet, illustrating the stalled migration. Simulations of this type can be run for many thousands of planetary orbits without any significant net inward migration occurring. Such systems are likely to be stable long after the circumbinary disk has dispersed, since the planets remain in the region of stability defined by the work of Holman & Wiegert (1999) and are probably the best candidates for finding stable circumbinary extrasolar planets. Interestingly, spectroscopic binary systems with significant eccentricity are significantly more numerous than those with lower eccentricities (Duquennoy & Mayor 1991; Mathieu et al. 2000), suggesting that circumbinary planets may be common if planets are able to form in circumbinary disks.

5 Conclusions

Much of the work presented in this article is preliminary, and so the following statements should be viewed with the necessary caution. The conclusions about planet formation and evolution in binary systems that we are able to draw thus far are:

- In systems such as γ Cep, the nascent circumstellar disk is expected to be tidally truncated at a radius of $\simeq 4$ AU, and to be driven into an eccentric and precessing state by the binary gravitational potential
- A low mass planet that forms in such a disk will itself become eccentric, and will migrate inward on a fairly rapid time scale
- Gas accretion onto such a planet is likely to be highly efficient because of the induced orbital eccentricity, such that a large fraction of the disk gas will accrete onto the planet. Simulations indicate that a gas disk containing $\simeq 3$ Jupiter masses will form a planet of $\simeq 2$ Jupiter masses, as required to fit the minimum mass of the planet detected in the γ Cep system.
- Simulations of planetesimals orbiting in a tidal truncated and eccentric protoplanetary disk indicate that high velocity collisions are likely. Such collisions will probably lead to fragmentation of the planetesimals rather than their growth. Further work is required to confirm this picture.
- Low mass planets in circumbinary disk migrate inward until they reach the gap edge, where they appear to stall due to the action of corotation torques.

- Should these low mass planets grow to become gas giants, a range of outcomes seem likely. These include stalled migration leading to the formatuon of stable circumbinary giant planets, and inward migration followed by scattering and ejection by the central binary.

References

Armitage, P. J., Clarke, C. J., & Tout, C. A. 1999, MNRAS, 304, 425
Artymowicz, P. & Lubow, S. H. 1994, ApJ, 421, 651
D'Angelo, G., Kley, W., & Henning, T. 2003, ApJ, 586, 540
de Val-Borro, M., Edgar, R. G., Artymowicz, P., et al. 2006, MNRAS, 370, 529
Duquennoy, A. & Mayor, M. 1991, A&A, 248, 485
Eggenberger, A., Udry, S., & Mayor, M. 2004, A&A, 417, 353
Hatzes, A. P., Cochran, W. D., Endl, M., et al. 2003, ApJ, 599, 1383
Holman, M. J. & Wiegert, P. A. 1999, AJ, 117, 621
Innanen, K. A., Zheng, J. Q., Mikkola, S., & Valtonen, M. J. 1997, AJ, 113, 1915
Kley, W. 1989, A&A, 208, 98
Kley, W. 1999, MNRAS, 303, 696
Kley, W. 2000, in IAU Symposium, 211P
Kley, W. & Burkert, A. 2000, in ASP Conf. Ser. 219: Disks, Planetesimals, and Planets, 189
Larwood, J. D., Nelson, R. P., Papaloizou, J. C. B., & Terquem, C. 1996, MNRAS, 282, 597
Lissauer, J. J., Quintana, E. V., Chambers, J. E., Duncan, M. J., & Adams, F. C. 2004, in Revista Mexicana de Astronomia y Astrofisica Conference Series, 99–103
Masset, F. S., Morbidelli, A., Crida, A., & Ferreira, J. 2006, ApJ, 642, 478
Mathieu, R. D., Ghez, A. M., Jensen, E. L. N., & Simon, M. 2000, Protostars and Planets IV, 703
Monin, J.-L., Clarke, C. J., Prato, L., & McCabe, C. 2007, in Protostars and Planets V, ed. B. Reipurth, D. Jewitt, & K. Keil, 395–409
Mugrauer, M., Neuhaeuser, R., & Mazeh, T. 2007, ArXiv Astrophysics e-prints
Mugrauer, M. & Neuhäuser, R. 2005, MNRAS, 361, L15
Nelson, A. F. 2000, ApJ, 537, L65
Nelson, R. P. 2003, MNRAS, 345, 233
Nelson, R. P., Papaloizou, J. C. B., Masset, F. S., & Kley, W. 2000, MNRAS, 318, 18
Neuhäuser, R., Mugrauer, M., Fukagawa, M., Torres, G., & Schmidt, T. 2007, A&A, 462, 777
Papaloizou, J. C. B. 2002, A&A, 388, 615
Papaloizou, J. C. B. 2005, A&A, 432, 757
Pierens, A., Dutrey, A., Guilloteau, S., & Huré, J.-M. 2005, in SF2A-2005: Semaine de l'Astrophysique Francaise, ed. F. Casoli, T. Contini, J. M. Hameury, & L. Pagani, 733–+
Pierens, A. & Nelson, R. 2007, MNRAS, 00, 00
Queloz, D., Mayor, M., Weber, L., et al. 2000, A&A, 354, 99
Quintana, E. V., Adams, F. C., Lissauer, J. J., & Chambers, J. E. 2007, ArXiv Astrophysics e-prints

Thébault, P., Marzari, F., Scholl, H., Turrini, D., & Barbieri, M. 2004, A&A, 427, 1097
Torres, G. 2007, ApJ, 654, 1095
Turrini, D., Barbieri, M., Marzari, F., Thebault, P., & Tricarico, P. 2005, Memorie della Societa Astronomica Italiana Supplement, 6, 172
Weidenschilling, S. J. 1977, MNRAS, 180, 57
Ziegler, U. & Yorke, H. 1997, Computer Physics Communications, 101, 54